Modal Analysis of X-Ray Laser Coherence

Richard A. London,[1] Moshe Strauss,[2] and Mordecai D. Rosen[1]

[1]*University of California, Lawrence Livermore National Laboratory, Livermore, California 94550*

[2]*Physics Department, Nuclear Research Centre–Negev, Beer Sheva 84190, Israel*

(Received 31 January 1990)

We present a modal analysis of the paraxial wave equation for plasma x-ray lasers. Gain guiding and refractive antiguiding are identified as the essential mechanisms which influence the coherence of the output radiation. Scaling laws for the number of guided modes and the coherence are given, depending on three parameters: the gain-dependent Fresnel number, the strength of refraction relative to gain, and the amplification length. The importance of controlling excess spontaneous emission to obtain coherence is identified. We suggest an experimental effort to verify various guiding regimes and to produce coherent output in the range between 45 and 200 Å.

PACS numbers: 42.50.Ar, 42.60.Da, 52.25.Nr

The rapid development of soft-x-ray lasers[1] and the intent to use them for holography[2] has stimulated much interest in their coherence properties. The longitudinal coherence required for holography should be easy to obtain, based on estimates of line profiles. Good transverse coherence appears to be more difficult to achieve.[3] Although there have been several previous studies of x-ray laser (XRL) propagation,[4,5] none have identified the physical mechanisms that influence the coherence properties of the output. In this paper, we identify gain guiding and refractive defocusing for a relatively small number of modes as the essential features of XRL transverse coherence. Deriving scaling laws and using semianalytical calculations, we demonstrate a way to reduce the number of guided modes and increase the coherence for several characteristic plasma profiles. We suggest experimental measurements toward the goal of a fully coherent XRL.

The wave-propagation problem in XRL's is similar to that in a broader class of mirrorless lasers. Discussions of the transverse coherence in superfluorescent[6] and stimulated Raman[7] sources have been reported. Propagator methods, expansions in free-space modes and orthogonal transverse modes, and numerical methods have been used to solve the wave equation.

We present a steady-state, wave-optics model describing the development of the radiation from spontaneous emission for arbitrary transverse profiles. Our method differs from the previous ones[5–7] in that we use a modal decomposition developed in recent papers on "excess spontaneous emission" in lasers,[8–10] and consider higher-order modes. The transverse modes are determined by the gain and refraction profiles, and are in general nonorthogonal.

We begin with the paraxial wave equation, including polarization by free electrons—a specific mechanism for refraction—and polarization by the atoms, causing spontaneous emission and gain:

$$\left[\frac{1}{k}\nabla_\perp^2 - 2i\frac{\partial}{\partial z} - h(\rho) + ig(\rho)\right]\mathcal{E}(\mathbf{r}) = -4\pi k\mathcal{P}_{\rm sp}(\mathbf{r}) . \quad (1)$$

Here $\mathcal{E}(\mathbf{r})$ is the complex slowly varying envelope of the electric field, specific to a unit bandwidth $d\omega$ at angular frequency ω. The free-space wave number is k, $\nabla_\perp$ is the transverse Laplacian, ρ is the transverse position vector, $h(\rho)\equiv\omega_p^2(\rho)/kc^2$ is the refraction strength, where ω_p is the electron plasma frequency ($\omega_p^2 \propto$ electron density), and $g(\rho;\omega)\equiv(4\pi^2 d^2 k/3\hbar)\psi_\omega\Delta N$ is the frequency-dependent gain coefficient, where d is the dipole matrix element for the laser transition, ΔN is the population inversion density, and ψ_ω is the normalized line-profile function ($\int\psi_\omega d\omega = 1$). We assume no gain saturation. The slowly varying envelope of the spontaneous atomic polarization $\mathcal{P}_{\rm sp}(\mathbf{r})$ is treated as a random function. Its correlation function is specified below in order to calculate observable quantities.

The electric field is written as a mode expansion: $\mathcal{E}(\mathbf{r}) = \sum c_n(z)u_n(\rho)$, allowing Eq. (1) to be separated into a transverse eigenvalue-eigenfunction ("mode") equation:

$$\left[\frac{1}{k}\nabla_\perp^2 - h(\rho) + ig(\rho)\right]u_n(\rho) = 2iq_n u_n(\rho) , \quad (2)$$

where q_n is an eigenvalue, and a first-order, longitudinal amplification equation for $c_n(z)$ (see Ref. 9, Eq. 3.8).

Equation (2) is identical to the time-independent Schrödinger equation, with a complex potential. The eigenfunctions are not orthogonal in the usual sense: $\int u_n u_m^* d\rho \neq \delta_{nm}$; rather, they obey the relationship $\int u_n u_m d\rho = \delta_{nm}$. Completeness can be shown for several transverse profiles. In some cases, continuum as well as discrete eigenfunctions are needed.

Observables of the radiation field may be found from the ensemble-averaged spatial correlation function $I_c \equiv \langle\mathcal{E}(\mathbf{r}_1)\mathcal{E}^*(\mathbf{r}_2)\rangle$. The radiation intensity $I(\mathbf{r})$ is proportional to $I_c(\mathbf{r}_1=\mathbf{r}_2)$. The transverse coherence is characterized by the absolute value of the complex degree of coherence:[11]

$$\mu(\rho_1,\rho_2;z) = |I_c(\rho_1,\rho_2;z)/[I(\rho_1;z)I(\rho_1;z)]^{1/2}| .$$

For $I(\rho_1;z)=I(\rho_2;z)$, μ (the "coherence function") gives the fringe visibility in a two-slit interferometer.

Given the mode expansion, I_c is written as a double sum over mode index:

$$I_c(\rho_1,\rho_2;z) = \sum_{n,m}\langle c_n(z)c_m^*(z)\rangle u_n(\rho_1)u_m^*(\rho_2) . \quad (3)$$

The correlation term ($\langle c_n c_m^* \rangle$) is found by formally solving the longitudinal equation for c_n and then constructing the ensemble average. We take the spontaneous-emission polarization to be δ-function correlated in space:[7,10]

$$\langle \mathcal{P}_{sp}(\mathbf{r}_1)\mathcal{P}_{sp}(\mathbf{r}_2)^* \rangle = [g(\omega)N_u \hbar/\Delta N \pi^2]\delta(\mathbf{r}_1 - \mathbf{r}_2),$$

where N_u is the density of atoms in the upper level. Assuming no incident radiation, we arrive at the following deterministic expression:

$$\langle c_n(z)c_m^*(z) \rangle = KB_{nm}[\exp(Q_{nm}z) - 1], \quad (4)$$

where $B_{nm} = \int u_n u_m^* d\rho$ are called overlap integrals, $Q_{nm} = q_n + q_m^*$, and $K = 4\hbar k N_u/\Delta N$. We have assumed that $N_u(\mathbf{r}) \propto \Delta N(\mathbf{r})$, and have used the relation $\int g u_n u_m^* d\rho = Q_{nm}B_{nm}$, derived from Eq. (2). Other assumptions about the upper-state profile would alter the B_{nm} factor in Eq. (4). The diagonal gain coefficient for the intensity in each mode is $g_n \equiv Q_{nn} = 2\mathrm{Re}(q_n)$. The overlap integrals are generally larger than unity, related to the excess spontaneous emission.[8-10] In principle, there is no difficulty in evaluating the double sum for the correlation function [Eq. (3)], despite the existence of off-diagonal overlap integrals.

The model equation (2) can be solved analytically for several cases. We rely on the usual solutions of the Schrödinger equation, generalized to complex potentials. We treat only the discrete part of the eigenfunction spectrum, and, for clarity, concentrate on problems with one transverse dimension.

First, we consider a square well because of its simplicity. The gain and (scaled) density have constant values g_0 and h_0, respectively, over a finite transverse range $-a < x < a$, and are zero outside. The eigenfunctions are

$$u_n(x) = \begin{cases} A_n(e^{i\alpha_n x} \pm e^{-i\alpha_n x}), & |x| \le a, \\ B_n e^{i\beta_n |x|}, & |x| > a. \end{cases} \quad (5)$$

Here α_n and β_n are complex, and are determined by the conditions that u_n and its first derivative be continuous at $x = \pm a$, and that the modes be discrete and localized (i.e., $u_n \to 0$ as $x \to \pm\infty$). Their determination requires the solution of a complex transcendental equation. The eigenvalues are given by $q_n = i(g_0/F_e)(\beta_n a)^2$, where $F_e \equiv k g_0 a^2$ is called the effective Fresnel number, obtained by substituting the e-folding length ($1/g_0$) for the laser length (L) in the usual formula for the Fresnel number ($F = ka^2/L$).

The solution space for the u_n's is two dimensional. In Fig. 1, we show the spectrum of gain coefficients for several cases of F_e and a refraction parameter $\eta \equiv h_0/g_0$. For each value of F_e and η there exists a finite number of discrete ("guided") modes. Approximate formulas for this number, valid for $F_e \gg 1$, are $n_g = 2F_e/\pi \ln[F_e/(1+\eta)]$ for $F_e/\eta \gg 2$, and $n_g = F_e^{3/4}\eta^{1/4}/\sqrt{2}$, for $F_e/\eta \le 2$. The slow increase in n_g with increasing η, due to reflection from the sharp boundaries at $x = \pm a$, is unrealistic for a plasma x-ray laser, but is applicable to hard-edged lasers.

The observables may be characterized by three parameters. We choose F_e, η, and a longitudinal parameter —the gain-length product, $G \equiv g_0 L$. The values of G range up to about 20, at which value gain saturation sets in.[4] The x dependence of the output intensity and the coherence function are shown in Fig. 2 for several cases. For relatively small F_e (and/or large G), the intensity is dominated by a few modes and their structure is apparent in the intensity. For large values of F_e, many modes contribute, producing a flat intensity distribution.

As F_e is decreased, the number of modes decreases (see Fig. 1) and so the degree of coherence increases. To characterize the fraction of coherent output, we define a coherence length L_{coh} as the distance from the center at which μ drops to $\frac{1}{2}$. We find for a wide range of parameters ($G = 5$–20, $F_e = 10$–1000, $\eta = 0$–50) that L_{coh} depends mainly on the Fresnel number F. We have fitted the results with the following scaling laws: $L_{coh} \approx 1.36 \times F^{-0.94}$ for $\eta = 0$, and $L_{coh} \approx 0.45F^{-0.76}$ for $\eta = 50$. With no refraction ($\eta = 0$), the scaling is close to the

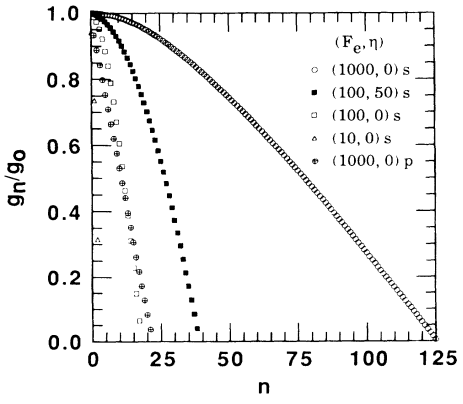

FIG. 1. Spectrum of diagonal gain coefficients for square (s) and parabolic (p) profiles.

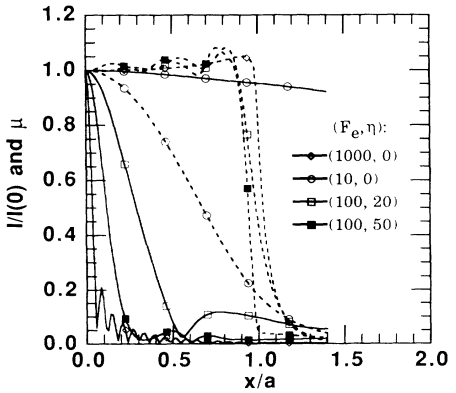

FIG. 2. Intensity (dashed curves) and coherence function (solid curves) vs transverse position for square profiles with $G = 20$.

F^{-1} law for an incoherent source propagating through free space.[7,11] We have understood the detailed behavior of L_{coh} from the scaling of the gain and the overlap integrals with mode index n.

The mode expansion converges for most parameter values considered for square profiles. We find, however, that due to increasing overlap integrals (excess emission), higher modes (approaching n_g) give increasingly larger contributions to the correlation function for small values of G and large values of F_e. For example, this occurs at $G<8$ for $F_e=1000$ and $\eta=50$. A correct calculation of the correlation function in these cases requires the inclusion of the continuum eigenfunctions, taking the limits of the paraxial approximation into account.

The second case which we consider is that of parabolic ("harmonic-oscillator") gain and density profiles, believed to be a reasonable model for the central region of exploding-foil x-ray laser.[4] Allowing for different widths of the profiles, we write $g(x)=g_0(1-x^2/a^2)$ and $h(x)=h_0(1-x^2/b^2)$. The eigenfunctions are the well-studied Hermite-Gaussian modes:[12]

$$u_n=A_nH_n((2\alpha)^{1/2}x)\exp(-\alpha x^2),$$

where H_n is the nth-order Hermite polynomial, $A_n=(2\alpha/\pi)^{1/4}(n!2^n)^{-1/2}$, $\alpha=ikp_0/2$, $p_0=[g_0(\eta-i)/ka^2]^{1/2}$, and $\eta=a^2h_0/b^2g_0$. The eigenvalues are $q_n=(g_0+ih_0)/2-p_0(n+\frac{1}{2})$, and the diagonal gain coefficients are $g_n=g_0[1-2\beta(n+\frac{1}{2})]$, where $\beta=(\mathrm{Re}p_0)/g_0$. The gains for $F_e=1000$ and $\eta=0$ are shown in Fig. 1. Expressions for the various parameters for weak and strong refraction are given in Table I. We note that the gain of the lowest mode ($n=0$) is the same as the effective gain derived from geometric optics in the strong-refraction limit.[4]

We identify guided modes as those localized in the region $|x|<a$. Only cases with $\mathrm{Re}(\alpha)a^2>1$ will have such modes, and for these, only the lower modes will be guided. Based on the quantum-mechanical analogy, we include only those modes whose gain is at least the gain decrement, $2\beta g_0$. They will behave like bound states in a potential well. When the eigenfunctions have appreciable amplitude for $|x|>a$, they become unrealistic because of the extension of parabolic profiles. Expressions for the number of guided modes valid for large numbers are given in Table I. In a plasma, refraction has the effect of bending rays outward and reducing the number of guided modes.

We have evaluated the overlap integrals for parabolic profiles with a recursion relation. The determination of the intensity and coherence function is complicated by the rapid increase of the overlap integrals (B_{nm}, or excess emission) with increasing mode number. For example, the diagonal terms scale approximately as 2.5^n for weak refraction, and as $(4\eta)^n$ for strong refraction. For large gainlengths, the increase of the overlap integrals may be offset by the decrease in the exponential amplification factor in Eq. (4), which scales like $[\exp(-2\beta G)]^n$. For example, the total power output, which is proportional to the transverse integral of intensity, scales like $\sim\sum(B_{nm})^2\exp(Q_{nm}z)$. The summation over modes will be well behaved if the higher-order terms give increasingly smaller contributions. This occurs for $F_e<1.25G^2$ for weak refraction and for $F_e<\eta G^2/[\ln(4\eta)]^2$ for strong refraction. For larger values of F_e, the growth of the terms with increasing mode number causes the correlation function to be dominated by the highest mode included. It appears necessary to cut off the summation in a manner consistent with the paraxial approximation.

TABLE I. Mode parameters for parabolic profiles.

Refractive case	$\mathrm{Re}(\alpha)a^2$	β	Number of guided modes 1D	2D
Weak ($\eta\ll1$)	$(F_e/8)^{1/2}$	$(1/2F_e)^{1/2}$	$(F_e/2)^{1/2}$	$F_e/4$
Strong ($\eta\gg1$)	$(F_e/\eta)^{1/2}/4$	$(\eta/F_e)^{1/2}$	$(F_e/4\eta)^{1/2}$	$F_e/8\eta$

To achieve a high degree of coherence two conditions must apply: There must be only a few guided modes (see Table I), and the excess emission in higher modes should not dominate, as expressed by the inequalities above.

The third case assumes inverse-cosh-squared profiles: $(g,h)\sim\cosh^{-2}(x/a)$. Such profiles go to zero at large $|x|$ as the square profiles and are smooth as the parabolic profiles. They are therefore more realistic models of an actual x-ray laser. The eigenfunctions can be expressed in terms of the hypergeometric function, while the eigenvalues are simple algebraic functions. The spectrum and number of guided modes are similar to those for the parabolic profiles (see Table I). The overlap integrals have been found in terms of the β function. We find for $\cosh^{-2}$ profiles, as well as for parabolic profiles, that the overlap integrals grow rapidly with increasing mode index for large F_e. We are able to model small F_e systems well and expect good coherence from them.

Lasers with rounded profiles (i.e., parabolic and $\cosh^{-2}$) have fewer guided modes and a higher degree of coherence than do those with the flat profiles (i.e., square well). This effect is caused by gain guiding and refractive antiguiding, both of which tend to favor radiation which travels straight down the center of the laser, where there is a local flatness of the profiles. The refractive mode-selecting effect would not be present in lasers with refractive guiding.

We apply our models to soft XRL's. For the Ne-like Se XRL,[13] we take the following typical parameters: wavelength $=210$ Å, $g_0=5\ \mathrm{cm}^{-1}$, $a=b=100\ \mu\mathrm{m}$, $n_e(0)=3\times10^{20}\ \mathrm{cm}^{-3}$, and lengths $L=1$–4 cm. The resulting parameters are $F_e=1500$, $\eta=59$, and $G=5$–20. This puts us in the strong-refraction regime. The saturation gainlength is expected to be very close to 20, depending only logarithmically on the atomic parameters.[4] Using

the square-profile model, we find 350 guided modes, a very flat intensity distribution across the face of the laser, and a coherence length of 1.5 μm. The output is not very coherent. To make a flat-profile laser coherent would require decreasing the width to about 10 μm. However, the density profiles are actually expected to be rounded. In the parabolic model, with $a=b=100$ μm, we find the modal gain coefficients $g_n=(4.0-2.0)n$. The diagonal overlap integrals scale approximately as 240^n. The validity condition for the convergence of the correlation function is violated even for the longest laser with $G=20$. To remain in the region of validity with $G\leq 20$ we would need $a\leq 67$ μm. In this case, a very coherent output is expected since only one or two modes are guided. With parabolic profiles, it appears that a rapid onset of coherence would occur as the laser is made narrower, entering the parameter region in which the lowest modes dominate the correlation function. An alternate method to make a coherent laser would be to choose $a<b$, by surrounding the lasant with another material. For example, keeping b fixed at 100 μm and choosing $a\leq 30$ μm gives high coherence, while satisfying the convergence requirement. The results for $\cosh^{-2}$ profiles are similar to those for the parabolic profiles.

For x-ray holography of biological samples, a wavelength near 44 Å appears optimal.[4] Amplification has recently been observed at 45 Å in Ni-like Ta.[14] Assuming typical parameters, $a=b=75$ μm, $g=2.5$ cm^{-1}, $n_e=10^{21}$ cm^{-3}, and L up to 4 cm, we have $F_e=2000$, $\eta=100$, and G up to 10. Longer lengths would be needed to saturate the laser at $G=20$. A square-profile laser would have $n_g=480$, and a very short coherence length, even at $G=20$. To get good coherence would require $a=b=5$ μm. For parabolic profiles, the required width is about $a=b=50$ μm for $G=20$, much easier to obtain.

We have presented an approach to improve XRL coherence by reducing the number of strongly amplified guided modes and limiting the excess spontaneous emission into higher modes. A theoretical effort should be conducted in order to understand the detailed scaling of the excess emission. We have presented scaling laws for the coherence in a variety of practical situations and have made suggestions to achieve good coherence in a few cases. A new experimental effort should be conducted in order to verify the scaling laws for the various guiding regimes and to obtain a coherent x-ray laser.

We thank N. Rostoker at University of California, Irvine, for his hospitality to M. Strauss during this work. We thank A. Shestakov for suggesting the recursive method for the parabolic overlap integrals, and P. Amendt, M. Feit, and J. Fleck for helpful discussions. This work was supported by the U.S. Department of Energy, Lawrence Livermore National Laboratory under Contract No. W-7405-ENG-48.

[1]For summaries of recent advances, see *Short Wavelength Coherent Radiation: Generation and Applications,* edited by R. Falcone and J. Kirz (Optical Society of America, Washington, DC, 1988); R. C. Elton, *X-Ray Lasers* (Academic, New York, 1990).

[2]R. A. London, M. D. Rosen, and J. E. Trebes, Appl. Opt. **28**, 3397 (1989).

[3]M. D. Rosen, J. E. Trebes, and D. L. Matthews, Comments Plasma Phys. Controlled Fusion **10**, 245 (1987).

[4]R. A. London, Phys. Fluids **31**, 184 (1988).

[5]M. Strauss, Phys. Fluids B **1**, 907 (1989); G. Hazak and A. Bar-Shalom, Phys. Rev. A **38**, 1300 (1988); **40**, 7055 (1989); E. E. Fill, Opt. Commun. **67**, 441 (1988).

[6]P. D. Drummond and J. H. Eberly, Phys. Rev. A **25**, 3446 (1982); J. Mostowski and B. Sobolewska, *ibid.* **30**, 1392 (1984).

[7]B. N. Perry, P. Rabinwitz, and M. Newstein, Phys. Rev. A **27**, 1989 (1983); J. Mostowski and B. Sobolewska, *ibid.* **30**, 610 (1984); M. G. Raymer, I. A. Walmsley, J. Mostowski, and B. Sobolewska, *ibid.* **32**, 332 (1985); I. A. Walmsley and M. G. Raymer, *ibid.* **33**, 382 (1986).

[8]K. Petermann, IEEE J. Quantum Electron. **15**, 566 (1979).

[9]H. A. Haus and S. Kawakami, IEEE J. Quantum Electron. **21**, 63 (1985).

[10]A. E. Siegman, Phys. Rev. A **39**, 1253 (1989).

[11]M. Born and E. Wolf, *Principles of Optics* (Pergamon, New York, 1970), 4th ed.

[12]For example, see D. Marcuse, *Light Transmission Optics* (Van Nostrand, New York, 1982).

[13]M. D. Rosen *et al.*, Phys. Rev. Lett. **54**, 106 (1985); D. L. Matthews *et al.*, *ibid.* **54**, 110 (1985).

[14]B. J. MacGowan *et al.*, Phys. Rev. Lett. **65**, 420 (1990).